

# EFFECT OF THE SHAPE OF IMPINGEMENT PLATE ON THE VAPORIZATION AND FORMATION OF FUEL MIXTURE IN IMPINGING SPRAY

J.-J. KANG<sup>1)</sup>, D.-W. KIM<sup>2)</sup>, G.-M. CHOI<sup>3)</sup> and D.-J. KIM<sup>3)\*</sup>

<sup>1)</sup>Research Institute of Mechanical Technology, Pusan National University, Busan 609-735, Korea

<sup>2)</sup>Graduate School of Mechanical Engineering, Pusan National University, Busan 609-735, Korea

<sup>3)</sup>School of Mechanical Engineering, Pusan National University, Busan 609-735, Korea

(Received 6 April 2005; Revised 28 February 2006)

**ABSTRACT**—The effect of the shape of the side wall on vaporization and fuel mixture were investigated for the impinging spray of a direct injection (DI) gasoline engine under a variety of conditions using the LIEF technique. The characteristics of the impinging spray were investigated under various configurations of piston cavities. To simulate the effect of piston cavity configurations and injection timing in an actual DI gasoline engine, the parameters were horizontal distance from the spray axis to side wall and vertical distance from nozzle tip to impingement plate. Prior to investigating the side wall effect, experiments on free and impinging sprays for flat plates were conducted and these results were compared with those of the side wall impinging spray. For each condition, the impingement plate was located at three different vertical distances ( $Z=46.7$ ,  $58.4$ , and  $70$  mm) below the injector tip and the rectangular side wall was installed at three different radial distances ( $R=15$ ,  $20$ , and  $25$  mm) from the spray axis. Radial propagation velocity from spray axis along impinging plate became higher with increasing ambient temperature. When the ambient pressure was increased, propagation speed reduced. High ambient pressures tended to prevent the impinging spray from the propagating radially and kept the fuel concentration higher near the spray axis. Regardless of ambient pressure and temperature fully developed vortices were generated near the side wall with nearly identical distributions, however there were discrepancies in the early development process. A relationship between the impingement distance ( $Z$ ) and the distance from the side wall to the spray axis ( $R$ ) was demonstrated in this study when  $R=20$  and  $25$  mm and  $Z=46.7$  and  $58.4$  mm. Fuel recirculation was achieved by adequate side wall distance. Fuel mixture stratification, an adequate piston cavity with a shorter impingement distance from the injector tip to the piston head should be required in the central direct injection system.

**KEY WORDS** : Direct injection spark ignition (DISI), Impinging spray, Laser induced exciplex fluorescence (LIEF), Vaporization, Vortex

## NOMENCLATURE

$I_a$  : accumulated intensity of a column in an acquired image  
 $I_k$  : measured intensity at Kth pixel [0-255]  
 $P_i$  : injection pressure [MPa]  
 $P_a$  : ambient pressure [MPa]  
 $h$  : spray height [mm]  
 $R$  : radial distance of side wall from spray axis [mm]  
 $r$  : radial distance from spray axis [mm]  
 $T_a$  : ambient temperature [K]  
 $t_i$  : elapsed time after injection start [ms]  
 $t_{inj}$  : injection duration [ms]  
 $Z$  : distance from injector tip to impingement plate [mm]

DISI : direct injection spark ignition  
 LIEF : laser induced exciplex fluorescence  
 SOI : start of injection  
 BTDC : before top dead center

## 1. INTRODUCTION

Stratified charge operation of a direct injection spark ignition (DISI) engine can improve fuel consumption under light loads due to reduced engine pumping loss, increased gas specific heat ratio, and a slight increase in knock limited compression ratio. The potential advantages are well known in terms of both fuel economy and efficient transient control (Iwamoto *et al.*, 1997). However, these advantages can be achieved by desirable mixture composition and local distribution inside a cylinder.

\*Corresponding author. e-mail: djkim@pusan.ac.kr

Fuel injection, evaporation and mixing should be artificially controlled in order to design advanced DISI engine because mixture formation is effected by complicated interactions among fuel spray (Araneo *et al.*, 2000; Choi *et al.*, 2002), flow motion (Kang and Kim, 2003) and chamber/piston geometry.

The interaction between the fuel sprays and cavity walls of piston has been an especially important issue in gasoline engines utilizing direct fuel injection. The amount of fuel wetting the walls (Park *et al.*, 1999; 2004) on the piston surface may increase, because the injected fuel spray during the latter stage of the compression stroke has a short travel length before impinging on the wall of the piston cavity. Therefore, it is important to investigate the interactions between the spray and the wall of the piston cavity.

To measure the spatial distribution of mixture concentration, a number of laser-based measurement techniques have been developed and used to study the vaporization and fuel-air mixture formation processes (Lee and Nishida, 2003) Though laser induced fluorescence (LIF) is a widely-used technique for measuring the concentration distribution of a spray, liquid and vapor phases cannot be distinguished by this technique. Recently, many researchers have used the LIF technique to obtain simultaneous images of the liquid and vapor phases in a DI gasoline spray (Ipp *et al.*, 1999). In an earlier study of DI gasoline spray, Preussner *et al.* (1998) suggested the basic mechanisms of the interaction between droplets and air over a hollow-cone spray. Senda *et al.* (1997) applied a LIEF technique to an impinging diesel spray, and quantitatively assessed vapor concentration by considering the quenching process of the fluorescence emission due to the mixture of temperature and vapor concentration.

However, a database that could be applied to a practical system has not been established, though the configuration of piston cavities plays a very important role on evaporation and mixture distribution as mentioned above. Therefore, it is important to investigate the characteristics and interactions between spray and cavity configuration of piston with various position.

In the present work, the characteristics of impinging spray were investigated under a variety of piston cavity configurations. To simulate the effect of piston cavity configurations and injection timing in practical DI gasoline engine, the following parameters were selected; the horizontal distance from the spray axis to the side wall and the vertical distance from the nozzle tip to the impingement plate. Furthermore, to analyze the effect of the cavity configuration and impingement distance from the nozzle tip, fundamental experiments were conducted on free and impinging sprays of a flat plate. The various configurations of the cavity and impingement distances were selected, based on these fundamental results. The

effect of side wall on the vaporization and mixture formation were investigated for impinging spray of DI gasoline using LIEF technique.

## 2. EXPERIMENTAL SETUP

Figure 1 shows a schematic of the experimental apparatus. LIEF was used to observe the liquid and vapor phase of impingement spray separately. The experimental setup includes a heated pressurized chamber designed for optical access, an aluminum plate with a side wall, and direct injection system.

Hexane was used as the fuel and a mixture of fluorobenzene and diethyl-methyl-amine (DEMA) was used as the tracer. The boiling points for hexane, fluorobenzene, and DEMA are 338 K, 342 K and 358 K, respectively, and the solution was composed of 89% hexane, 2% fluorobenzene and 9% DEMA by volume.

The fourth harmonic of the Nd:YAG at 266 nm with duration of 7 ns was used to excite dopants from the fuel sprays. The laser beam formed a thin light sheet of 60 mm high and less than 400  $\mu\text{m}$  thick. The filters were  $300\pm 25$  nm for vapor phase and  $400\pm 25$  nm for liquid phase. An additional WG280 sharp cut filter was used to eliminate the light at 266 nm.

The spray images were digitally recorded with an intensified CCD camera that provided 640 by 480 pixel images at a resolution of 8 bits and was mounted perpendicular to the laser sheet. The camera system consisted of a personal computer with an image grabber, a shutter controller, and a pulse generator. In order to inject the fuel with high pressure and to avoid pressure fluctuations in the fuel rail, a compressed nitrogen cylinder and hydraulic accumulator were used. A high pressure swirl injector with  $60^\circ$  was used. The injection pressure and duration were kept at 5.1 MPa and 2.0 ms for all experimental conditions. The position of the injector and configuration of the impingement plate are shown in

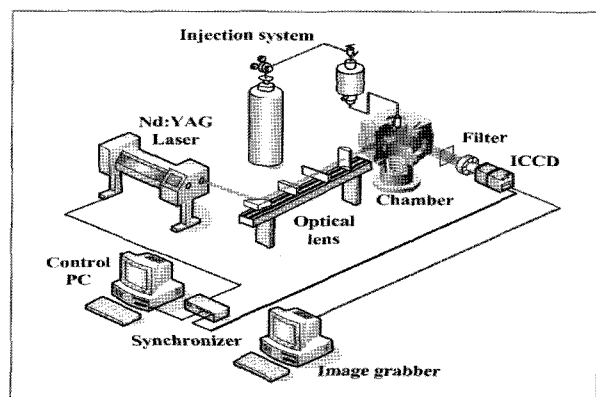


Figure 1. Schematic of experimental setup.

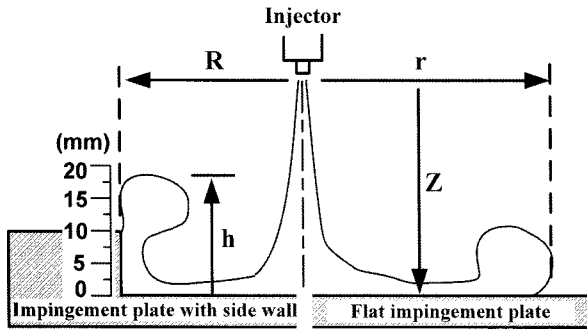


Figure 2. The position of the injector and configurations of the impingement plate.

Table 1. Experimental conditions.

Injection pressure, $P_i$ [MPa]	5.1
Injection duration, $t_{inj}$ [ms]	2.0
Ambient pressure, $P_a$ [MPa]	0.1, 0.3, 0.5
Ambient temperature, $T_a$ [K]	293, 373, 473
Radial distance of side wall from spray axis, $R$ [mm]	15, 20, 25
Distance of impingement plate from injector tip, $Z$ [mm]	46.7, 58.4, 70

Figure 2.

For each condition, the aluminum plate was located at three different vertical distances ( $Z=46.7, 58.4, 70$  mm) from the nozzle tip to the impingement plate and the rectangular side wall was installed at three different horizontal distances ( $R=15, 20, 25$  mm) from spray axis. Experimental conditions are shown in Table 1. The impingement distance and radial distance to side wall from spray axis corresponds to the crank angle and cavity radius in a DI gasoline engine, respectively.  $Z=46.7, 58.4$  and  $70$  mm correspond to BTDC  $60^\circ, 75^\circ$  and  $90^\circ$ , respectively.

### 3. RESULTS AND DISCUSSION

#### 3.1. Effect of Ambient Pressure and Temperature on Vaporization and Mixture Formation in Free Spray

Before the interaction between spray and piston cavity could be investigated, it is important to have a detailed understanding of the spray characteristics. Figure 3 shows the influence of the ambient pressure and temperature on the spray formation and vaporization in free spray. The injector nozzle was located at the center of the upper side of the images. The images were taken at  $1.6$  ms after start of injection (SOI).

A laser sheet passed through the spray axis. The swirl injector produced a hollow cone spray structure, which

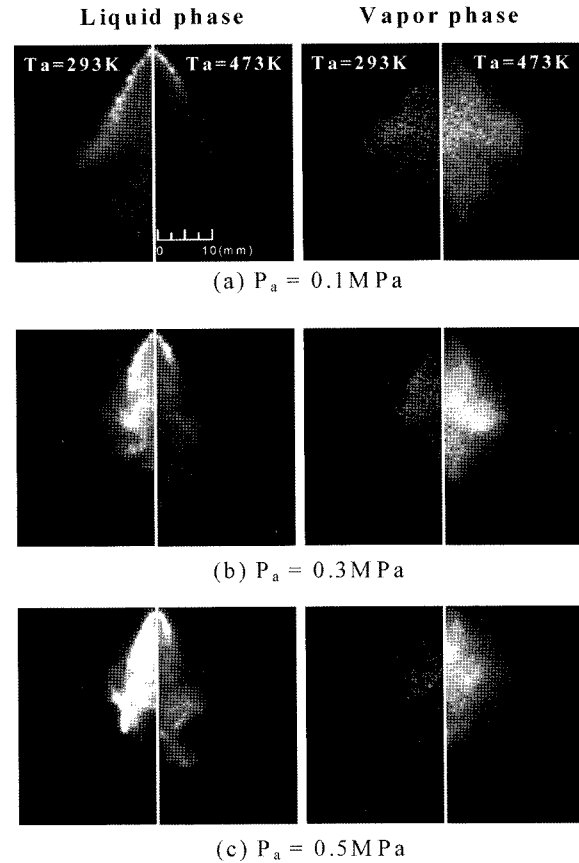


Figure 3. Fluorescence images of liquid and vapor phases with different ambient pressure and temperature.

was preceded by a “pre-jet”. As the ambient pressure is increased, the spray angle of the hollow cone and penetration is decreased, hence the spray became compact and a merged structure was observed. When the ambient temperature was high and the ambient pressure low, droplets were rapidly vaporized at the spray tip, and with high ambient pressure, the intensity of the vapor phase at the inner region of the spray core was rather high. From the above results, we can see that low ambient temperatures and high ambient pressures prevented the spray from active evaporation and mixing the air and fuel respectively.

#### 3.2. Effect of Impinging Spray on the Flat Plate

To investigate the characteristics of the impinging spray, measurement by LIEF method was taken on the flat plate.

Figure 4 shows the fluorescence images of the impinging spray for the flat plate taken at  $3$  ms after SOI with different ambient pressures ( $P_a=0.1$  MPa,  $0.3$  MPa, and  $0.5$  MPa) and temperatures ( $T_a=293$  K,  $373$  K, and  $473$  K). The distance,  $Z$ , from injector tip to flat plate was set to  $46.7$  mm.

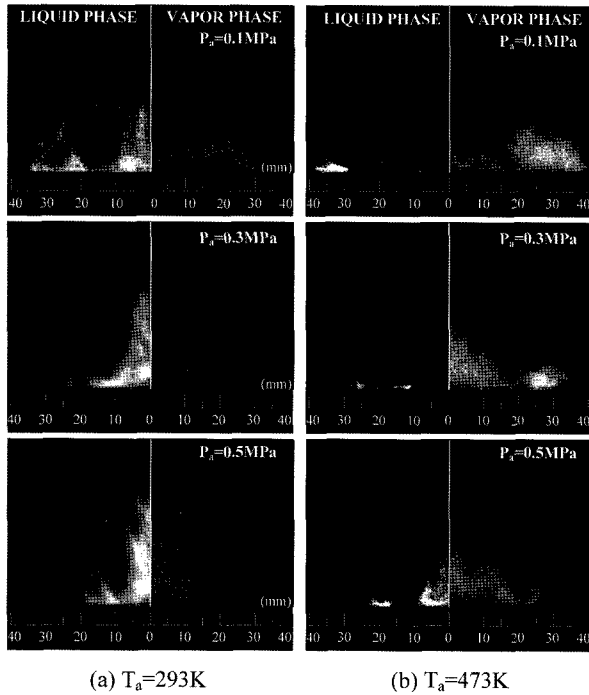
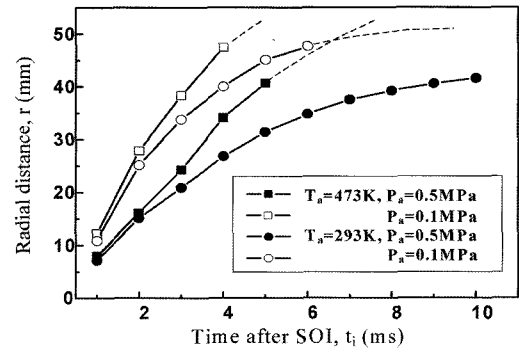


Figure 4. The fluorescence images of the impingement spray on the flat plate.

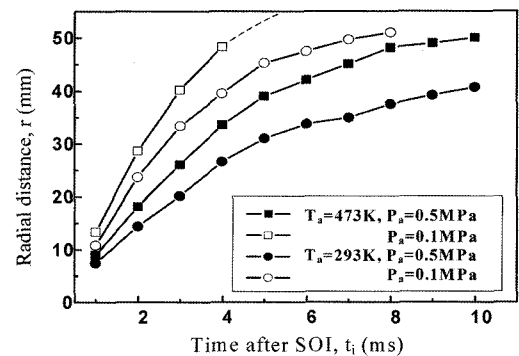
With increasing ambient pressure, both liquid and vapor phases concentrated toward spray axis at ambient temperature of 293 K. A relatively slow propagation speed was also observed near nozzle tip as the ambient pressures increased. These tendencies were similar to those of the free spray. The vortex of the spray tip propagated radially along the impingement plate. A recirculation region was clearly observed being formed by impingement. It is thought that most small droplets are entrained to the inner spray cone by this recirculation.

Though the liquid phase intensity was rather high at low ambient temperature, the vapor phase intensity could obviously be observed at high temperatures, which resulted from rapid evaporation. For high ambient temperatures, most of the liquid phases appeared only on the plate regardless of ambient pressure and vaporization was enhanced. The liquid phase near the wall, which was not vaporized on impingement plate yet, quickly propagated radially. The above results demonstrate that the ambient temperature plays an important role in vaporization just after the impingement.

Figure 5 shows the radial distance of the impinging spray tip from the spray axis as a function of elapsed time after SOI. When ambient temperature was high and ambient pressure was low, the vapor and liquid phases propagated radially more quickly from the spray axis along the wall. Because high ambient temperatures caused enhanced evaporation, liquid phase did not last more than



(a) Liquid phase



(b) Vapor phase

Figure 5. Radial distance of impingement spray tip from spray axis as elapsed time after SOI.

4 ms after the start of injection. The above results demonstrate that ambient pressures dominate radial propagation speed of the impinging spray.

Figure 6 shows accumulated radial intensity of vapor phases as a function of ambient pressure and temperature respectively. The images, show propagation up to 40 mm from the spray tip, were captured for each condition.

Accumulated intensity,  $I_a$ , can be expressed as follows

$$I_a = \sum_{K=0}^Z I_K,$$

where,

$Z$  : distance from nozzle tip to impingement plate.

$I_k$  : measures the intensity at  $K$ th pixel, and

$I_a$  : accumulated intensity of a column in an acquired image.

An ambient temperature of 293 K had monotonously low accumulated intensities at the spray tip independent of ambient pressures. Conversely, as ambient temperature increased, bimodal distribution of accumulated intensity was observed and this tendency was dominant at higher ambient pressures. These bimodal distributions of accumulated intensity resulted from recirculation toward

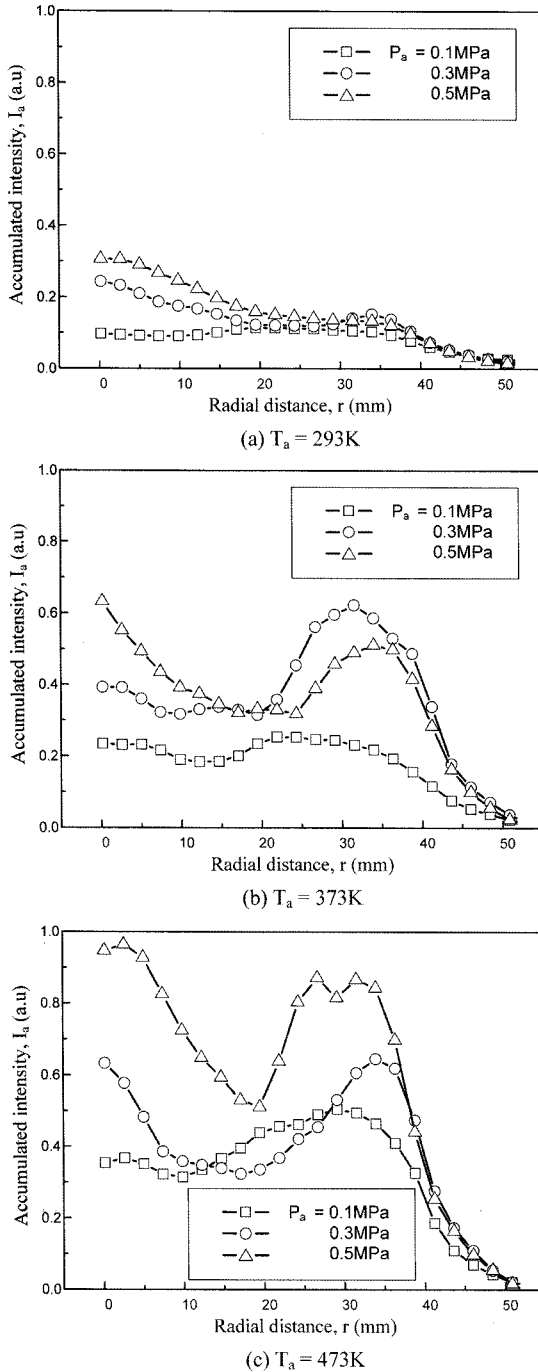


Figure 6. Radial accumulated intensity on ambient pressure at 3.0ms after SOI.

the spray axis. We can see that the spatial distribution of the vapor phase is controllable with ambient temperatures and pressures after impinging on the plate.

### 3.3. Effect of Impinging Spray with a Side Wall

Figure 7 shows fluorescent images of a vapor phase with

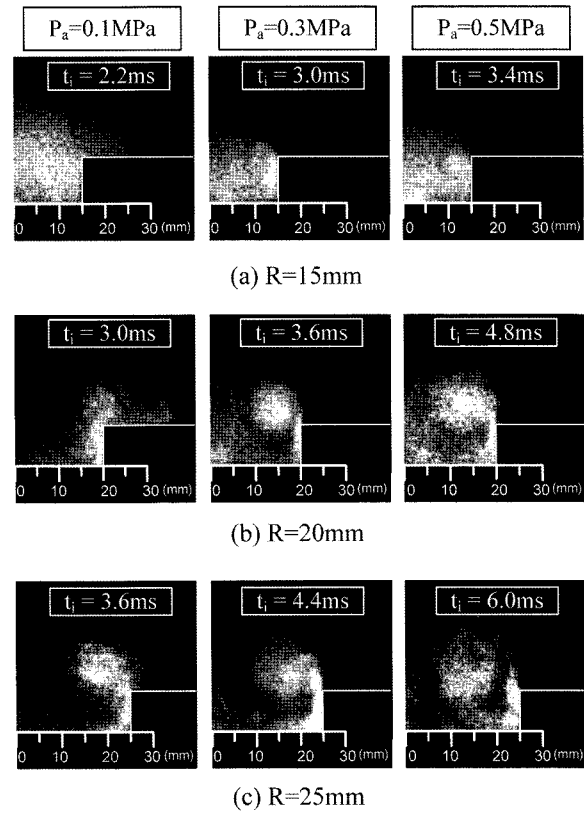
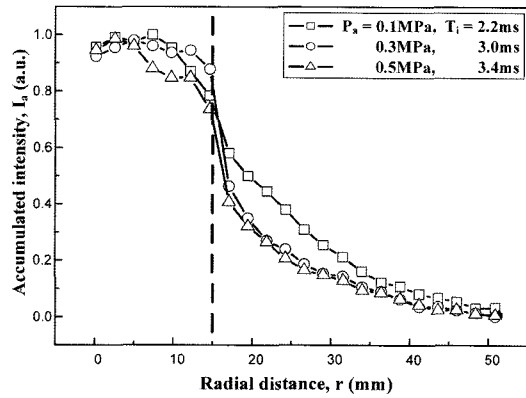


Figure 7. The fluorescence image on the behavior of the vapor phase with different radial distance of the side wall.

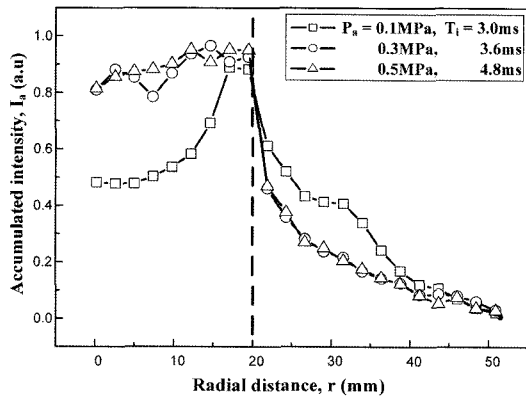
the various radial distances to the side wall from the spray axis at ambient temperature of 473 K. Each condition had a different propagation velocity because of the differing cavity diameters. Based on arrival times, 1.8 times elapsed images are shown in Figure 7. The spray radii are 30, 18 and 15 mm for 0.1, 0.3 and 0.5 MPa, respectively, and the distance from injector tip to impingement plates when the ambient pressure was 0.1 MPa, part of vapor phase existed at outside of side wall because of the large spray radii ( $R=15$  mm and 20 mm).

As the ambient pressure increased, and the impinged spray tip propagated outward, it generated a recirculation zone near the side wall.

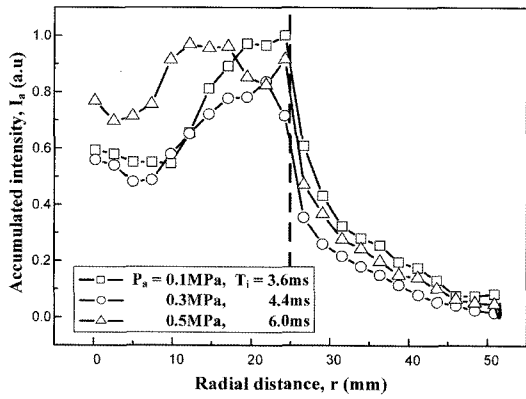
Figure 8 shows the accumulated vertical intensity of the vapor phase at ambient temperature of 473 K that was used to investigate its distribution in detail. The accumulated intensity was non-dimensionalized by maximum intensity for each condition. Dots in figures indicate the position of the side wall. Regardless of ambient pressure, bimodal distribution was not observed with a radial distance of 15 mm. However, the vapor phase was present in the side wall as ambient pressure increased. This is resulted from a wider spray radius at low ambient pressure.



(a) R=15mm



(b) R=20mm

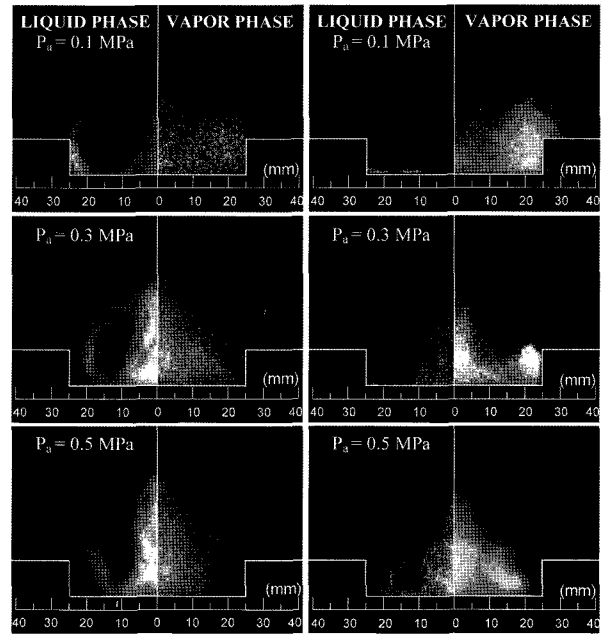


(c) R=25mm

Figure 8. Radial accumulated intensity of the vapor phase with different radial distance of the side wall.

When the radius was narrow and the ambient pressure low, parts of the injected spray seemed to impinge on the side wall directly. As the radius ( $R$ ) increased, bimodal distribution was observed under ambient pressures of 0.3 and 0.5 MPa.

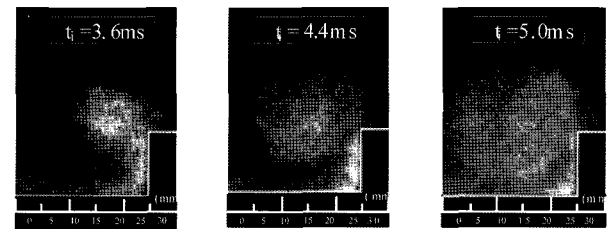
Figure 9 shows the fluorescent images that were used to investigate the effect of side wall on vaporization and



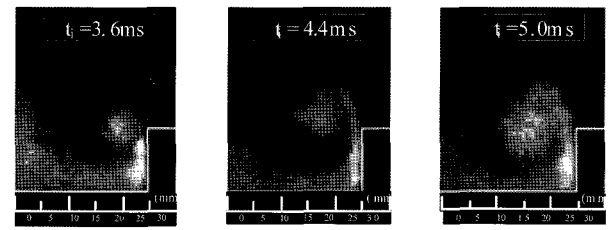
(a)  $T_a=293K$

(b)  $T_a=473K$

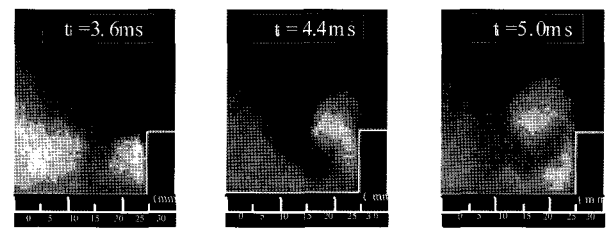
Figure 9. The fluorescence images of the impingement spray on the plate with side wall at 3 ms after SOI.



(a)  $P_a = 0.1 MPa$



(b)  $P_a = 0.3 MPa$



(c)  $P_a = 0.5 MPa$

Figure 10. The fluorescence images on the behavior of spray tip with different ambient pressure as the time elapses ( $T_a=473 K, R=25 mm$ ).

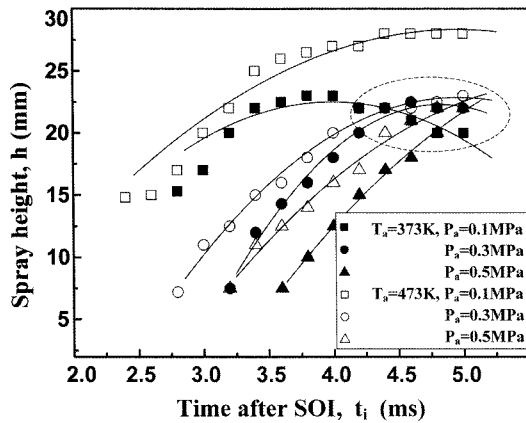


Figure 11. Effect of ambient pressure and temperature on spray height.

spray behavior of the impinging spray on plates with side walls with different ambient pressures. Figure 10 shows the time series spatial distributions of the vapor phase under different pressures. The radius of 25 mm was used because almost all of the vapor phase existed inside the side wall. In Figure 9, it is well known that vaporization was enhanced as ambient temperature increased and propagation and diffuse of vapor phase speed increased.

Conversely, vaporization and propagation speed were suppressed when ambient pressure increased. These tendencies are quite similar to those of the impinging spray on a flat plate. In Figure 10, the injector nozzles were located at the left upper side of the images. Though the spatial distributions of vapor phases differed according to the different ambient pressures for the same time interval after SOI, the qualitative trends of development were similar regardless of the ambient pressure. Rapid diffusion of the vapor phase was apparent at ambient pressure of 0.1 MPa.

Figure 11 shows the heights of vapor phase that were obtained under various ambient pressures and temperatures. These were used to investigate the development of vortices near the side wall. The fuel at the spray tip diffused rapidly in the air when the ambient pressures were low and ambient temperatures were high. Therefore, the spray heights were high in the early stages when ambient pressures were low and temperatures were high. However, most of the vapor phase vortices generated near the side wall reveals nearly the same height (20 mm), where spray height was defined as the distance from the spray tip to bottom impingement plate. Spray heights were closed to each other at 4.5 ms SOI regardless of ambient pressure and temperature although there were discrepancies in the early development process except when temperature was 473 K and pressure was 0.1 MPa. In the most of ambient condition, spray height didn't increase any more with the lapse of time at around

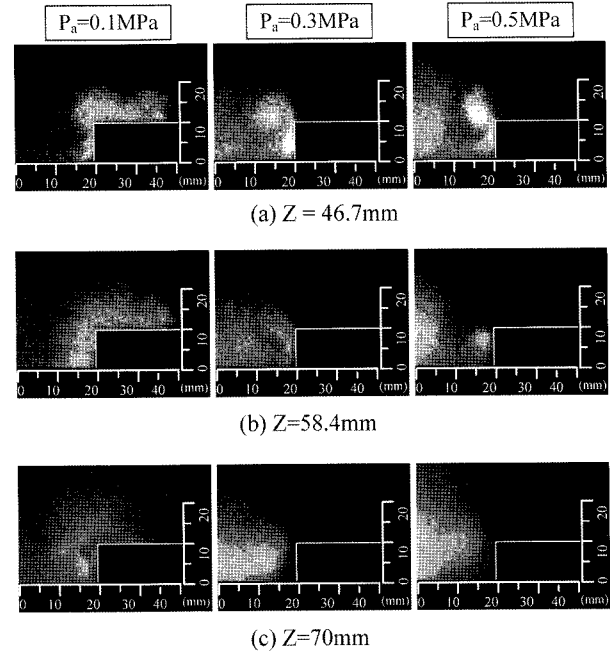


Figure 12. The fluorescence image of the vapor phase with different impingement distance from injection tip at 3.6 ms after SOI ( $T_a=473$  K,  $R=20$  mm).

4.5 ms SOI because spray tip was entrained inner spray cone.

The effect of impingement distance was also investigated. Figure 12 shows a typical fluorescent image of the vapor phase as a function of impingement distance ( $Z$ ) from the injection tip when  $R=20$  mm at 3.6 ms after SOI. The impingement distance corresponds to the crank angle in a DI gasoline engine. When ambient pressure was 0.1 MPa, parts of the vapor phase existed outside of the side wall even at large impingement distances. As ambient pressure increased, impinging spray formed a recirculation zone by the side wall. However, recirculation by the side wall was not observed for long impingement distance ( $Z=70$  mm) and most of the vapor phase was concentrated near the spray axis. This is ascribed to the rapid vaporization and mixing of air and fuel before arrival at the impingement plate. From this we can deduce that there was a large dissipation of energy.

The relationship between impingement distance ( $Z$ ) and side wall distance ( $R$ ) from the spray axis was investigated. Figure 13 shows the accumulated intensity distribution as functions of impingement distance, distance from the side wall to the spray axis, ambient pressure, and an ambient temperature of 473 K. When ambient pressure was 0.1 MPa, the vapor phase exceeded the side wall under all conditions, which indicates that it is difficult to control fuel distribution by side wall and impingement distance. When ambient pressure was 0.3

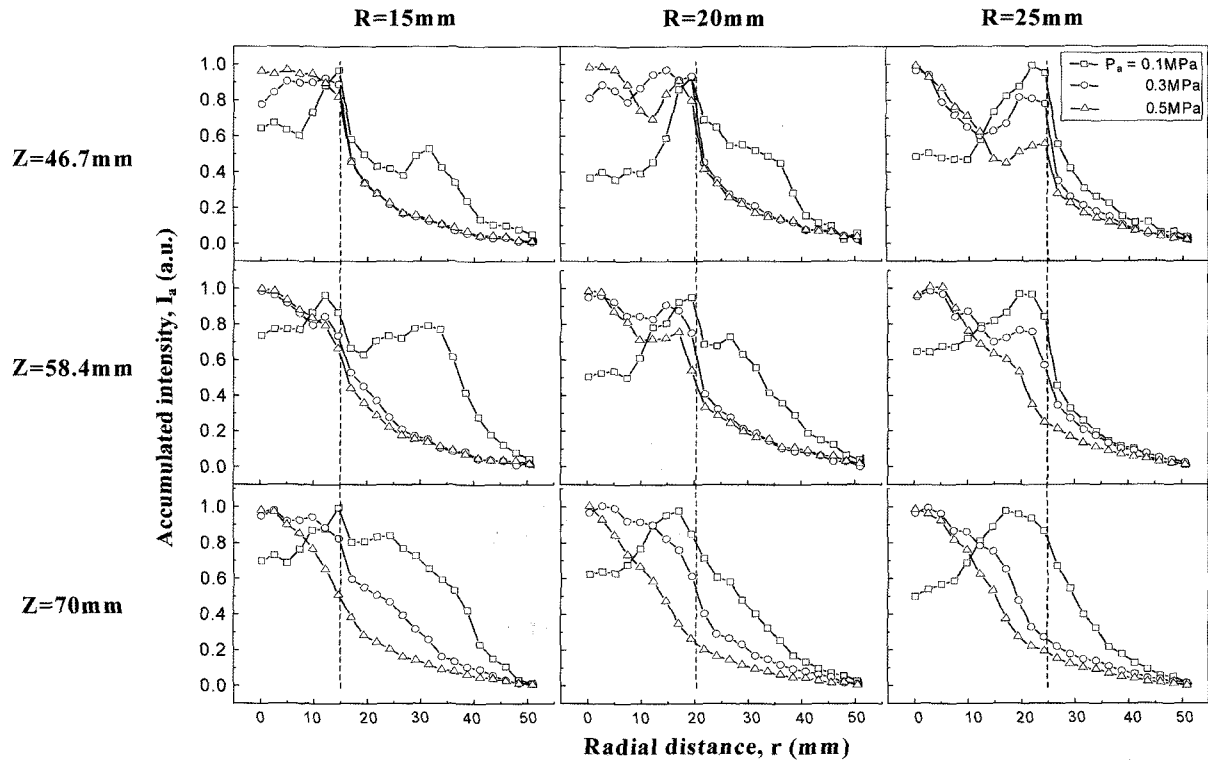


Figure 13. The accumulated radial intensity of the vapor phase with different impingement distance from injection tip and radial distance of side wall from spray axis at 3.6 ms after SOI.

and 0.5 MPa, we observed bimodal distribution inside the side wall for  $R=20$  and 25 mm. This result indicates that a short distance from side wall to spray axis restricts fuel recirculation.

For long impingement distances ( $Z=70$  mm), though bimodal distribution was not observed, which indicates that for recirculation to be near the side wall, the injected fuel concentrated near the spray axis under relatively high ambient pressure. This result indicates that ambient pressure is dominated for long impingement distance condition than side wall distance. From the above results, the relationship between the impingement distance and side wall distance from spray axis was demonstrated, which was informative regarding fuel stratification. An adequate piston cavity with a shorter length of impingement distance from the injector tip to the piston head should be required in the type of the central direct injection system.

#### 4. CONCLUSIONS

The characteristics of impinging spray were investigated for various configurations of piston cavities, such as side wall distance and impingement distance, under different ambient and impingement conditions using LIEF technique. Through this study on evaporation and mixture

formation of the impinging spray, the following results have been obtained:

- (1) When ambient temperatures were high without impingement of the spray on the plate, droplets at the spray tip rapidly evaporated under low ambient pressure. As ambient pressure increased, intensity of the vapor phase was rather high in the inner region of the spray cone.
- (2) Radial propagation from the spray axis during the vapor and liquid phases was faster along the impingement plate when ambient temperatures were high than when low. As ambient pressure increased, radial propagation slowed. High ambient pressure tended to prevent impinging spray from propagating radially and concentrate fuel near the spray axis.
- (3) In the development of vortices, the spray heights converged on 20 mm from impinging plate except 473 K of temperature and 0.1 MPa of pressure condition.
- (4) A relationship between impingement distance ( $Z$ ) and the distance from the side wall to the spray axis ( $R$ ) was demonstrated in this study. Fuel recirculation was achieved when  $R=20$  and 25 mm and  $Z=46.7$  and 58.4 mm, which are adequate impingement and side wall distances.
- (5) For fuel mixture stratification, an adequate piston



cavity with shorter impingement distance from the injector tip to the piston head should be required in the type of the central direct injection system.

## REFERENCES

- Araneo, L., Coghe, A., Brunello, G. and Donde, R. (2000). Effects of fuel temperature and ambient pressure on a GDI swirled injector spray. *SAE Paper No.* 2000-01-1901.
- Choi, D. S., Choi, G. M. and Kim, D. J. (2002). Spray structures and vaporizing characteristics of a GDI fuel spray. *J. Mechanical Science and Technology* **16**, **7**, 999–1008.
- Iwamoto, Y., Noma, K., Nakayama, O., Yamauchi, T. and Ando, H. (1997). Development of gasoline direct injection engine. *SAE Paper No.* 970541.
- Ipp, W., Wagner, V., Kramer, H., Wensing, M. and Leipertz, A. (1999). Spray formation of high pressure swirl gasoline injectors investigated by two-dimensional Mie and LIEF techniques. *SAE Paper No.* 1999-01-0498.
- Kang, J. J. and Kim, D. J. (2003). Effects of piston shapes and intake flow on the behavior of fuel mixtures in a GDI engine. *J. Mechanical Science and Technology* **17**, **12**, 2027–2033.
- Lee, J. K. and Nishida, K. (2003). Simultaneous flow field measurement of D.I. gasoline spray and entrained ambient air by LIF-PIV technique. *SAE Paper No.* 2003-01-1115.
- Park, J. S., Xie, X., Im, K. S., Kim, H. S., Lai, M-C., Yang, J., Han, Z. and Anderson, R. W. (1999). Characteristics of direct injection gasoline spray wall impingement at elevated temperature conditions. *SAE Paper No.* 1999-01-3662.
- Park, J. S., Im, K. S., Kim, H. S. and Lai, M. (2004). Visualization and measurement of a narrow-cone DI gasoline spray for the impingement analysis. *Int. J. Automotive Technology* **5**, **4**, 221–238.
- Preussner, C., Doring, C., Fehler, S. and Kampmann, S. (1998). GDI: Interaction between mixture preparation, combustion system and injector performance. *SAE Paper No.* 980498.
- Senda, J., Kanda, T., Kobayashi, M. and Fujimoto, H. (1997). Quantitative analysis of fuel vapor concentration in diesel spray by exciplex fluorescence method. *SAE Paper No.* 970796.